

FEATURES OF THE PREPARATION AND STUDY OF ELECTROPHYSICAL CHARACTERISTICS (BeO + TiO₂)-CERAMICS BY IMPEDANCE SPECTROSCOPY

A. A. Lepeshev,¹ A. V. Pavlov,¹ N. A. Drokin,^{2,3} A. I. Malkin,⁴
V. S. Kiiko,^{4,5} and N. S. Knyazev⁴

Translated from *Novye Ogneupory*, No. 6, pp. 55 – 63, June, 2019.

Original article submitted March 4, 2019.

An electrically conducting two-component BeO-ceramic with the addition of micro- and nano-crystalline TiO₂ powder is prepared that can be used as a material for scattered microwave radiation absorption in high-power electronic devices. The nature of the occurrence of electrical conductivity and absorption of the microwave field in (BeO + TiO₂)-ceramics is not completely established. Impedance spectroscopy is used for the first time to investigate the electrical and dielectric characteristics of this ceramic in the frequency range from 100 Hz to 100 MHz in relation to presence of micro- and nano-sized TiO₂ phase within the BeO ceramic composition. It is established that the static resistance of ceramics with addition of a TiO₂ nanopowder is significantly reduced compared with the resistance of original ceramic with TiO₂ micropowder. It is shown that real and imaginary components of the dielectric constant of the ceramic studied increase to abnormally large values with a reduction in frequency of the effective electric field, and in the high frequency range $f \geq 10^8$ Hz the process of dielectric relaxation commences leading to an increase in dielectric loss angle. Dielectric properties of ceramic samples are determined under blocking conditions for through conduction. The effect of TiO₂ micropowder additions on dielectric polarization processes with frequency increasing up to 12×10^9 Hz is considered.

Keywords: (BeO + TiO₂)-ceramic, electrophysical properties, impedance, frequency dependence, dielectric permittivity, dielectric loss tangent.

INTRODUCTION

Recently considerable attention has been devoted to synthesis and study of nano-phase high-temperature ceramics with increased density, thermal conductivity, special structures, and electrophysical properties, useful for electronic engineering and instrument building [1 – 6]. There is special interest in BeO-ceramic, whose electrical properties may undergo marked changes with addition to the composition of

TiO₂ micropowder in an amount of 5 – 40 wt.% [2, 4 – 6]. This ceramic is used in electronic engineering instruments of considerable power as a material for absorption of scattered UHF-radiation. The effect of adding TiO₂ nano-powder on the properties of these absorbents has not been studied. It has been established by experiment that the absorbing properties of (BeO + TiO₂)-ceramic are due to many factors, primarily its electrical conductivity. In the original condition BeO-ceramic exhibits a high melting temperature $\sim 2547^\circ\text{C}$, good thermal conductivity (280 – 320 W/(m·K)) and is classified as dielectric with considerable width of the inhibition zone (~ 10.8 eV) with a volumetric specific resistance $\rho \sim 10^{15}$ Ω·cm at room temperature [3]. Dielectric permittivity ϵ of pure BeO-ceramic has a value of 6.9 – 7.2, and the dielectric loss at frequency 1 MHz does not exceed a value of $\text{tg}\beta = 3 \times 10^{-4}$ [2 – 4].

¹ FGBOU VO Siberian Federal University, Krasnoyarsk, Russia.

² FGBUN Federal Research Center, Krasnoyarsk Scientific Center, Siberian Section of the Russian Academy of Sciences, Krasnoyarsk, Russia.

³ FGBOU VO Academician M. F. Reshetnev Siberian Aerospace University, Krasnoyarsk, Russia.

⁴ FGAOU VO Ural Federal University, Ekaterinburg, Russia.

⁵ v.kijko@mail.ru

During synthesis of ceramic with added TiO_2 there is a change in density in the range $2.8 - 3.2 \text{ g/cm}^3$ and a reduction in thermal conductivity in the range $150 - 65 \text{ W/(m}\cdot\text{K)}$ [4]. If after sintering additional calcining of ceramic is conducted in a reducing atmosphere (CO or H_2) at 1480°C for $1.5 - 2.9 \text{ h}$, the specimens obtained become electrically conducting with specific conductivity within the limits from 8×10^{-8} to $4 \times 10^{-1} (\Omega\cdot\text{cm})^{-1}$ [5]. A similar increase in conductivity also occurs with direct sintering of BeO and TiO_2 powders in a vacuum in furnaces with a graphite lining, graphite heaters, and a graphite charge in the range $1450 - 1540^\circ\text{C}$ [6]. Heat treatment of ceramic in a CO atmosphere leads to a stronger increase not only in conductivity, but also in capacity to absorb UHF-radiation in the gigahertz frequency range [7, 8].

Beryllium oxide of low-temperature modification ($\alpha\text{-BeO}$) under normal conditions crystallizes in a structure of the wurtzite type, formed by dense hexagonal packing of oxygen ions with tetragonal and octahedral vacancies [9]. Beryllium ions occupy half the tetrahedral cavities and form a hexagonal sub-lattice. TiO_2 pertains to the class of oxides of transition metals and has several modifications, in this case it is rutile, which exhibits a tetragonal crystal structure. The valent zone of TiO_2 is formed by external p -electrons of oxygen, and the bottom of the conductivity zone is predominantly with excited titanium ions [10]. The particular value for electronic properties of TiO_2 of special importance for electronic properties is the rutile modification explained by presence of partly reduced titanium (Ti^{3+}), whose level is at about $0.2 - 0.8 \text{ eV}$ below the bottom of the conductivity zone [11]. These zones are in the form of donors, leading an electron type of conductivity. Presence of Ti^{3+} also determines conductivity of the titanium oxide obtained, whose specific resistance decreases from a value of 10^7 to $10^2 \Omega\cdot\text{cm}$ [12].

During sintering of $\text{BeO} + \text{TiO}_2$ in furnaces with carbon heaters in a graphite charge there is probably introduction of carbon into the region of ceramic, which may affect the value of conductivity. According to results of x-ray photoelectron spectroscopy it has been established that at boundaries between BeO crystals in the presence of TiO_2 micro- or nano-particles an established crystalline phase may arise exhibiting both conducting and dielectric properties.

The electrophysical properties of this ceramic have hardly been studied. Conducting layers, arising at the surface of crystals, lead to a complex path for current carrier movement, which may depend on frequency and magnitude of an alternating electric field applied to a specimen. Mobile charges may accumulate at the boundaries of individual crystals and this may facilitate development of internal inhomogeneous electric fields, complicating the process of current carrier movement and relaxation. The main task of this work is treatment of manufacturing technology for experimental specimens of BeO -ceramic with addition of micro- and nano-crystalline TiO_2 phase and a study of the effect of additions on electro-transfer and polarization of this ce-

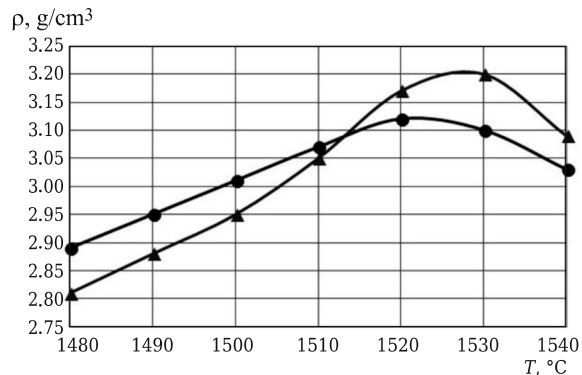


Fig. 1. Dependence of apparent density ρ on ceramic specimen sintering temperature: \blacktriangle) $\text{BeO} + 30 \text{ wt.}\% \text{ TiO}_2$ (μm); \bullet) $\text{BeO} + 20 \text{ wt.}\% \text{ TiO}_2$ (μm) + $1 \text{ wt.}\% \text{ TiO}_2$ (nano).

ramic by the method of measuring impedance in the frequency range from 100 Hz to 100 MHz .

CERAMIC FORMATION AND SINTERING

The starting specimen of a two-component ceramic used was of the composition $\text{BeO} + 30 \text{ wt.}\% \text{ TiO}_2$. In order to prepare this ceramic by plant technology fired BeO powder was used with an average crystallite size of $1.0 - 1.5 \mu\text{m}$ and TiO_2 micron powder (TU 6-10-727-78) with the same particle size. Then $1 \text{ wt.}\%$ of nanodispersed micron TiO_2 powder (size $30 - 50 \text{ nm}$) prepared in a plasma chemical low-pressure reactor [14] was added to the micro powder.

Specimens of BeO -ceramic were prepared with addition of $30 \text{ wt.}\% \text{ TiO}_2$ powder of micron size and $20 \text{ wt.}\%$ of micron size, to which $1 \text{ wt.}\%$ of TiO_2 nano-powder was added.

The starting components for a $\text{BeO} + \text{TiO}_2$ charge were mixed in a specially developed reactor of the impeller type in distilled water under conditions of continuous bubbling with compressed air. Then slip mixes were prepared based on organic binder: wax, paraffin, oleic acid from calculation of loss during calcining of 9.5% . A wax-paraffin binder built in the ratio, wt.%: paraffin 82, wax 15, oleic acid 3. Workpiece molding was carried out in a unit for thermoplastic slip casting. The specimens obtained were round in cross section in the form rod 12 mm in diameter and 20 mm long. After burning off the organic binder and sintering specimens in a reducing atmosphere (in a graphite charge using a rough vacuum furnace with carbon heaters) rods were cut with a diamond tool to a diameter of $7.0_{-0.1} \text{ mm}$ and sliced into disks $1_{-0.1} \text{ mm}$ thick. Technology for preparing both types of ($\text{BeO} + \text{TiO}_2$)-ceramic with micron powder and with addition TiO_2 nano-powder coincided.

The optimum sintering temperature regime was selected for the maximum of apparent density and crystal size. The furnace was heated with each step of 100°C/h in the range $1480 - 1540^\circ\text{C}$, held at the maximum temperature for 1 h , cooled to 1200°C under load, and then natural cooling. With

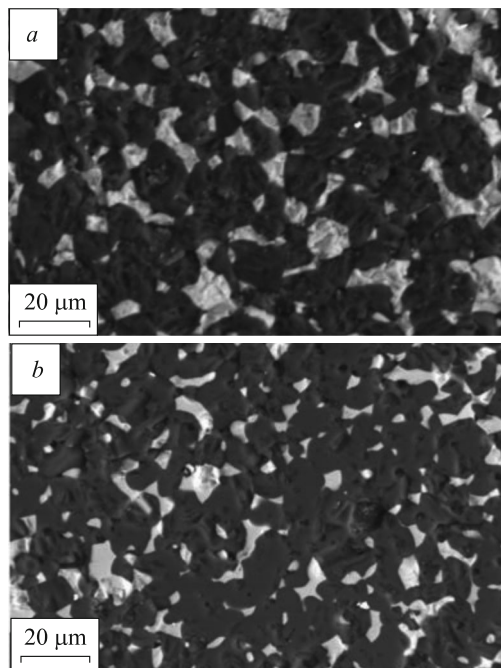


Fig. 2. Specimen microstructure: *a*) BeO + 30 wt.% TiO₂ (μm); *b*) BeO + 20 wt.% TiO₂ (μm) + 1 wt.% TiO₂ (nano). TiO₂ is light, BeO is dark.

an increase in sintering temperature specimen density ρ increases in direct proportion to sintering temperature. On reaching 1520°C a maximum is observed for ρ (3.2 g/cm³) for specimens with TiO₂ micron powder. A further increase in sintering temperature for these specimens leads to a reduction in ρ . This agrees with data in [15] where it was shown that introduction into BeO-ceramic of micron TiO₂ in an amount of 5, 10, 20, and 30 wt.% under identical thermodynamic conditions during sintering is accompanied by an increase in ρ from 2.8 to 3.2 g/cm³. With addition of 1 wt.% TiO₂ nano-powder to the composition BeO + 20 wt.% TiO₂ (micron) the maximum ρ for specimens did not exceed 3.12 g/cm³. In order to achieve the result obtained for determining the closed density of specimens in relation to sintering temperature density was analyzed in ten different specimens of the same batch of powders. The mean square deviation of density values did not exceed 1%.

The microstructure of experimental specimens was studied in a JSM-6390LV scanning electron microscope with an energy microanalysis attachment (Fig. 2).

Ceramic of the composition BeO + 30 wt.% TiO₂ (μm) is a mechanical mixture of quite coarse TiO₂ inclusions (see Fig. 2*a*). Within the structure non-uniform distribution of TiO₂ micro-crystals is observed with formation of comparatively coarse accumulations. In this case TiO₂ structural elements tend towards a rounder shape, and areas of grouped crystallites are also observed. Within specimens of ceramic with addition nano-particles the TiO₂ structural elements have a significantly smaller sizes, and in this case fine and

extended fragments are observed. TiO₂ nano-powder wets the surface of BeO micro-crystals by flowing over the surface (see Fig. 2*b*). Melting limits the rate of BeO micro-recrystallization.

BERYLLIUM CERAMIC IMPEDANCE SPECTROSCOPY

The electrophysical properties of BeO + 30 wt.% TiO₂ (μm) and BeO + 20 wt.% TiO₂ (μm) ceramics with addition of 1 wt.% TiO₂ (nano) have been compared. Measurement of the frequency dependence for impedance for the specimens obtained was performed in an Agilent E5061B spectrum analyzer in the frequency range from 10 Hz to 100 MHz. The essence of this method includes determining electrophysical properties of composite materials in relation alternating voltage frequency, applied to electrodes, between which there is a specimen. Measurement of impedance modulus $|Z|$ is based on determining numerous values of alternating current flowing through a specimen. Simultaneously the shift in phases between current and voltage is recorded [16].

In order to measure impedance characteristics of the ceramic obtained at end surface of specimens 7.0_{-0.1} mm in diameter and 1_{-0.1} thick a thin (~0.2 mm) layer of indium was rolled, which was pressed to the specimen surface with a miniature screw clamp in order to provide stable contact with direct and alternating currents. By means of needle-shaped pins a cell was prepared with ceramic connected to the impedance meter and the frequency dependence of impedance $|Z|$, and phase shift angle between current and voltage were recorded in an electronic recorder. Then frequency dependences were calculated for the actual ($Z' = |Z| \cdot \cos\varphi$) imaginary ($Z'' = |Z| \cdot \sin\varphi$) components of impedance that made it possible to determine the main complex electrophysical of test material (Fig. 3).

Results are provided in Fig. 3 for measurement of the frequency dependence of impedance modulus $|Z|(f)$ and phase shift angle $\varphi(f)$ between current and voltage for two of the ceramic specimens prepared.

For a specimen with addition of micron TiO₂ powder (see Fig. 3*a*) $|Z|$ in the low-frequency region $f \sim 10^3$ Hz has a value of about 4.3 kΩ and with an increase in frequency to $f \sim 10^8$ Hz it decreases uniformly to 3.6 Ω. The phase frequency characteristic of ceramic starts almost from zero, since at low frequencies through a specimen only the active component of current passes, determined by material static resistance. With an increase in electric field frequency a reactive (capacitive) component of current develops, and therefore φ increases to -82° at a frequency of 10^6 Hz (see Fig. 3*a*). With a further increase in frequency gain there is a reduction in φ to -47° at a frequency of 10^6 Hz. For ceramic containing TiO₂ nano-particles (see Fig. 3*b*) the low frequency values of $|Z|$ decrease considerably and are 830 Ω.

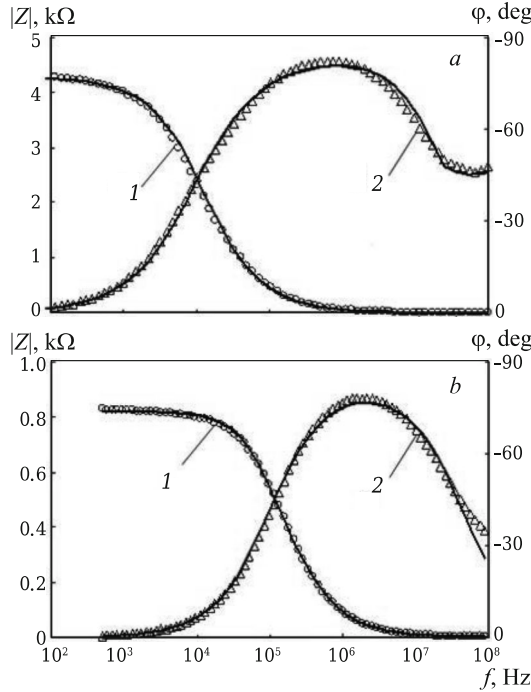


Fig. 3. Frequency relationships $Z(f)$ and $\phi(f)$ (light markers) for two ceramic specimens: *a*) with 30 wt.% TiO_2 (μm); *b*) with 20 wt.% TiO_2 (μm) with added 1 wt.% TiO_2 (nano). Solid lines are results of impedance spectra approximation by means of equivalent electric circuits (Fig. 4).

The phase angle for frequencies $f = 10^3$ Hz always equals zero, although at frequencies $f > 10^5$ Hz the nature of the behavior of $|Z|(f)$ and $\phi(f)$ is almost identical to the preceding specimen.

In the impedance method for analysis of the resistive-capacitive properties of the test substances and for understanding electrophysical processes occurring within them a procedure was adopted of construction of suitable electric circuits, whose impedance agrees with an experiment. Different radio engineering elements of these circuits may be modelled not only the internal part of a specimen but also surface properties and even an interface arising in some cases close to electrical contacts. For these ceramic speci-

mens by means of a special iso-analyzer program the most suitable equivalent circuits were selected (see Fig. 4). Results of numerical approximation of impedance spectra by means of these equivalent circuits are shown in Fig. 3 by solid lines.

Both circuits contain normal radio engineering elements R -resistance and C -capacitance. In these circuits a linear dependence is present for parameters, the artificial constant phase element (CPE), which to some extent reflects the electrical properties of the different structural inhomogeneous materials themselves. Impedance (Z_{CPE}) of this element is written in the following form [17]:

$$Z_{\text{CPE}} = \frac{1}{A(i\omega)^\eta} = \frac{1}{A\omega^\eta} \left[\cos\left(\eta \frac{\pi}{2}\right) - i \sin\left(\eta \frac{\pi}{2}\right) \right], \quad (1)$$

where A is a numerical multiple; ω is angular frequency; i is imaginary unit; η is exponent, determining the nature of impedance frequency dependence ($-1 \leq \eta \leq 1$).

A CPE element has both active and imaginary components. For whole values $\eta = 1, 0, -1$ a CPE element degenerates to normal C, R, L , elements. Fraction values of the exponent $\eta < 1$ formally specify a material cluster structure.

The simplest electrical circuit for ceramic with TiO_2 nano-powder (see Fig. 4a) contains three elements in all: resistance $R_1 = 2.9 \Omega$, $R_2 = 827 \Omega$, and element CPE_1 with a numerical multiple $A_0 = 5.32 \times 10^{-9}$ and exponent close to one, $\eta = 0.92$. A smaller amount of resistance in a circuit for a specimen with addition of TiO_2 nano-powder, as will be shown subsequently, facilitates an increase in specific conductivity, dielectric loss angle and dielectric permittivity. It may be noted that resistance R_2 almost coincides with the value of low-frequency impedance $|Z|$ of the given ceramic (830 Ω) and naturally models ceramic static resistance. Resistance $R_1 = 2.9 \Omega$ in the radio frequency region and remains almost unchanged, although with an increase in frequency, when specimen impedance decreases, this resistance contributes a perceptible contribution to formation of the impedance spectrum. In particular, this resistance in the region of high and possibly ultra-high frequencies leads to an impedance observed in the spectrum with a

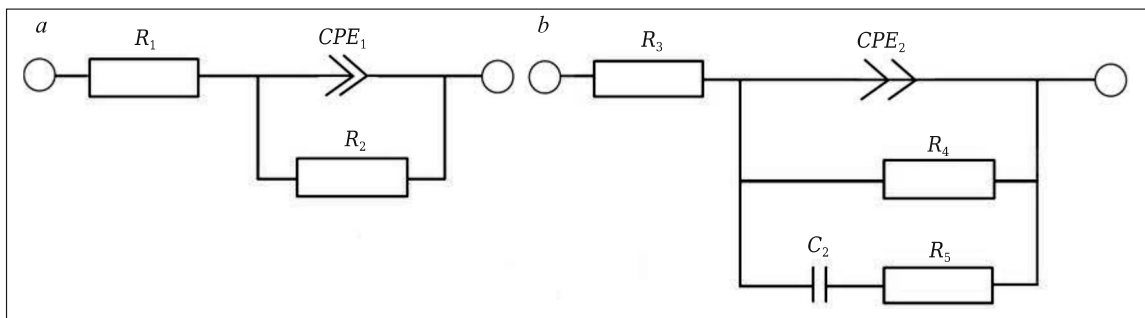


Fig. 4. Equivalent circuit for specimens: *a*) $\text{BeO} + 20 \text{ wt.}\% \text{TiO}_2$ (μm) + 1 wt.% TiO_2 (nano); *b*) $\text{BeO} + 30 \text{ wt.}\% \text{TiO}_2$ (μm).

reduced phase for alternating current passing through a specimen.

For a ceramic specimen with added micron TiO₂ powder the frequency dependence of impedance is shown in Fig. 3a, and the equivalent circuit is shown in Fig. 4b. This circuit of more complex and apart from the CPE₂ element contains parallel circuits one of which consists of resistance $R_4 = 4300 \Omega$, modeling ceramic static resistance. The second circuit was formed successively by include elements $C_2 = 2.9 \times 10^{-8} \text{ F}$ and $R_5 = 4 \Omega$, which form impedance characteristics in the medium frequency region. A CPE₂ element has a numerical multiple $A_0 = 2.9 \times 10^{-8}$ and exponent $n = 0.72$. This exponent signifies that the CPE₂ element may be treated as frequency-dependent capacitance and simultaneously is frequency-dependent resistance. Resistor R_3 , as for the preceding specimen, serves for modeling the high-frequency electrical losses. In order to model impedance in the decimetre and centimetre ranges of wavelength it is possible to make use of additional elements.

The cluster structure of this conducting ceramic is also reflected also in such electrophysical material characteristics as specific conductivity and dielectric permittivity. According to experimental measurements the impedance spectrum calculations were made of the active and imaginary components of specific conductivity (σ' , σ'') and dielectric permittivity (ϵ' , ϵ'') in accordance with the following equations [18] (Fig. 5)

$$\sigma'(\omega) = Y'(\omega) \frac{d}{S} = \frac{Z'(\omega) d}{|Z(\omega)|^2 S}; \quad \sigma''(\omega) = Y''(\omega) \frac{d}{S} = \frac{-Z''(\omega) d}{|Z(\omega)|^2 S}; \quad (2)$$

$$\epsilon'(\omega) = \frac{-Z''(\omega) d}{\epsilon_0 \omega |Z(\omega)|^2 S}; \quad \epsilon''(\omega) = \frac{Z'(\omega) d}{\epsilon_0 \omega |Z(\omega)|^2 S}, \quad (3)$$

where $Y'(\omega)$ and $Y''(\omega)$ are active and imaginary components of ceramic admittance; d is test ceramic plate thickness; S is contact area of cell measured capacitance; ϵ_0 is vacuum dielectric permeability.

In the low frequency region $f \leq 10 - 10^5 \text{ Hz}$ σ' of specimens depends little on frequency and is 5.1×10^{-3} (see Fig. 5a) and $2.7 \times 10^{-2} \Omega^{-1} \cdot \text{m}^{-1}$ (see Fig. 5b). However, in the frequency range $f \sim 10^4 - 10^8 \text{ Hz}$ σ' for both specimens increases uniformly by more than two orders of magnitude. The imaginary component of conductivity $\sigma''(\omega)$ for both ceramic specimens increases with an increase in frequency almost linearly, and it is determined by their value of effective capacitance $\sigma''(\omega) = \omega \cdot C$. However, on approach to frequency $f \sim 100 \text{ MHz}$ there is a tendency towards deviation from linearity in view of development of high-frequency dispersion of dielectric permittivity for specimens and their capacitance. The dielectric loss angle $\text{tg}\delta$ for a specimen with micron TiO₂ powder (see Fig. 5a) is at a minimum at frequency $f = 1 \text{ MHz}$, where the reactive component of conductivity (curve 2) predominates over the active component

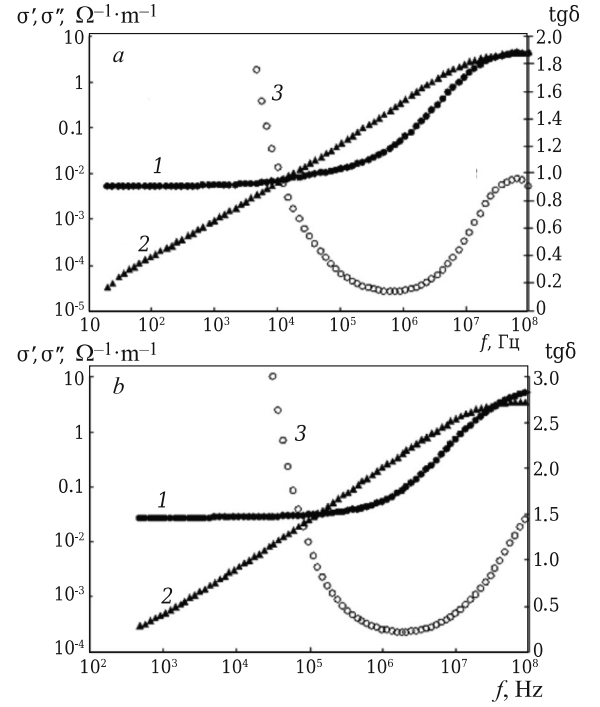


Fig. 5. Frequency dependence of actual σ' (1) and imaginary σ'' (2): a) specimen of composition BeO + 30 wt.% TiO₂ (μm); b) specimen of composition BeO + 20 wt.% TiO₂ (μm) + 1 wt.% TiO₂ (nano). Frequency dependences are given on the right axis for dielectric loss angle $\text{tg}\delta$ (3).

(curve 1). The maximum of $\text{tg}\delta$ for this ceramic appears during approach to frequency $f \sim 100 \text{ MHz}$. At this frequency σ' becomes comparable with σ'' (see Fig. 5a). In a specimen with nano powder the maximum $\text{tg}\delta$ is probably found at frequencies $F > 100 \text{ MHz}$, and at this frequency has a value of 1.5 (see Fig. 5b).

In order to explain possible reasons for an increase in σ' with an increase in frequency numerical approximation of electrical spectra was performed by means of a universal relationship [9]:

$$\sigma'(\omega) = \sigma_{\text{dc}} + a \cdot \omega^s, \quad (4)$$

where σ_{dc} is a steady-state value of conductivity; a is a numerical coefficient; s is exponent, $0 < s \leq 1$.

For a specimen with micron size TiO₂ powder (see Fig. 5a, curve 1) an exponent $s = 0.094$ was obtained, which is close to one and points to conductivity that is accomplished by overflow of current carriers from one conductive mass to another. However, the formal value of $s < 1$ may point to presence of jumping conductivity, arising either within clusters or between clusters. This conductivity is possible with presence of titanium ions with different valency. The possibility of existence of a volume of valency between a homological series of titanium oxides with the possibility

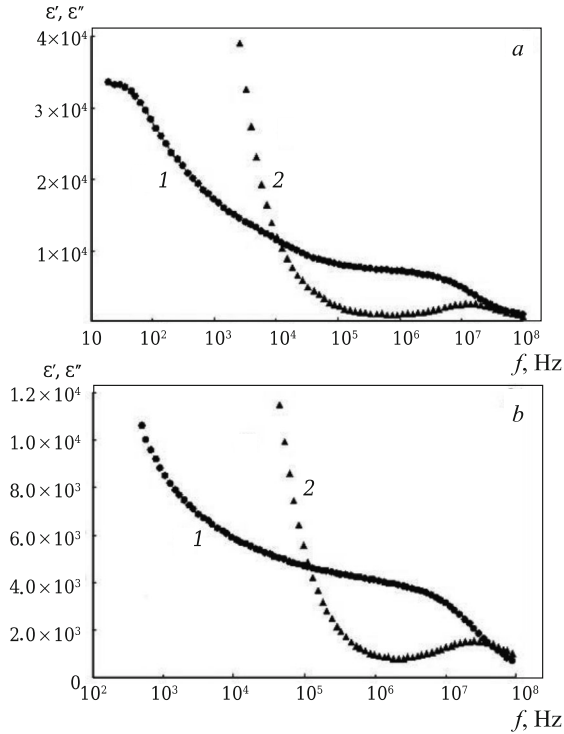


Fig. 6. Frequency dependences of ε' (1) and ε'' (2): *a*) specimen of composition BeO + 30 wt.% TiO₂ (μm); *b*) specimen of composition BeO + 20 wt.% TiO₂ (μm) + 1 wt.% TiO₂ (nano).

of vacancies according to oxygen has been considered in [20].

With approximation of conductivity for a specimen with TiO₂ nano-powder (see Fig. 5*b*, curve 1) by Eq. (4) the exponent reaches a value of $s = 1.96$, which entirely excludes jumpwise conductivity. Through conductivity of this ceramic is probably realized due to overflow or tunnelling of the charge carrier between conducting participants at the surface of TiO₂ nanoparticles. At the same time individual conducting islands may arise that are isolated from each other. In this case at low frequency there is a shift in charges towards the boundaries of these islands, which is accompanied by an increase in the degree of local polarization and an increase in active components of dielectric permittivity ε' . With an increase in frequency the shift in charges starts to lag behind the external field with respect to phase, and an additional relaxation component arise that gives an increase in exponent in expression (4) almost to $s = 2$ and leads to an increase in $\text{tg}\delta$. Frequency dependences for the active ε' and imaginary ε'' component of dielectric permittivity of the test specimens are shown in Fig. 6.

The enormous values of ε' and ε'' observed in the low-frequency region often arise in very different structurally inhomogeneous materials with conducting clusters due to accumulation of charges at their boundaries. The electric field of these charges screens the external field within a spec-

imen and this is perceived in an experiment as an apparent increase in ε [21].

An increase in ε'' is mainly due to presence of through conductivity and is determined by the following equation [22]

$$\varepsilon''(\omega) = \frac{\sigma'(\omega)}{\varepsilon_0 \omega}, \quad (5)$$

where ε_0 is an electric constant.

Within the limit $\omega \rightarrow 0$, $\varepsilon''(\omega) \rightarrow \infty$ with an increase in frequency the process of charge accumulation does not arise and the dielectric permittivity tends towards a steady value ε_∞ . The frequency dependences of ε' and ε'' decrease with an increase in frequency, but at even at high frequency $f \sim 10^7 - 10^8$ Hz they have an enormous values of 760 and 220 respectively (see Fig. 6). This signifies that the process of dielectric relaxation embraces a region of ultrahigh frequencies and is accompanied by absorption of a UHF-field [23].

The high values of ε' and ε'' revealed are not actual material parameters, but some effective values arising due to non-uniform distribution of electric charges and a field within a substance. More correct results of measuring dielectric properties are obtained in the average frequency region $f \geq 10^6$ Hz where relaxation maxima start to appear in frequency dependences $\varepsilon''(\omega)$ in the frequency region $10^7 - 10^8$ Hz (see Fig. 6). It is not excluded that in other ceramic specimens in relation to synthesis production regime dielectric relaxation absorption of electric field energy may occur at higher frequencies in the UHF region.

In the low-frequency region actual dielectric properties of test ceramic are distorted by presence of free charges and through conductivity. However, it is possible to obtain a more real representation of the electrophysical properties of this ceramic if the maximum effect of through conductivity on dielectric spectra is avoided. A method has been proposed in [24] for separating actual dielectric and relaxation characteristics of conducting heterogeneous materials, based on analyzing data for dispersion of a complex dielectric module. In certain cases this approach makes it possible to obtain important information about electric and relaxation properties of materials. In this work another method is proposed for determining low-frequency dielectric characteristics of ceramic specimens, implemented under conditions when one of the metal electrodes of the measuring cell is insulated from the specimen surface by a thin dielectric layer. This layer blocks a through electric current for a specimen and a more real representation may be obtained about the value of frequency of the ε' and ε'' dependences. For this a thin dielectric layer of Teflon was placed between one of the metal electrodes at a specimen. The thickness of the layer (10 μm) was selected in order that the capacitance of the condenser with the layer ($C_{\text{tefl}} = 1 \times 10^{-10}$ F) exceed the cell with composite actual capacitance. In this case during subsequent connection of these

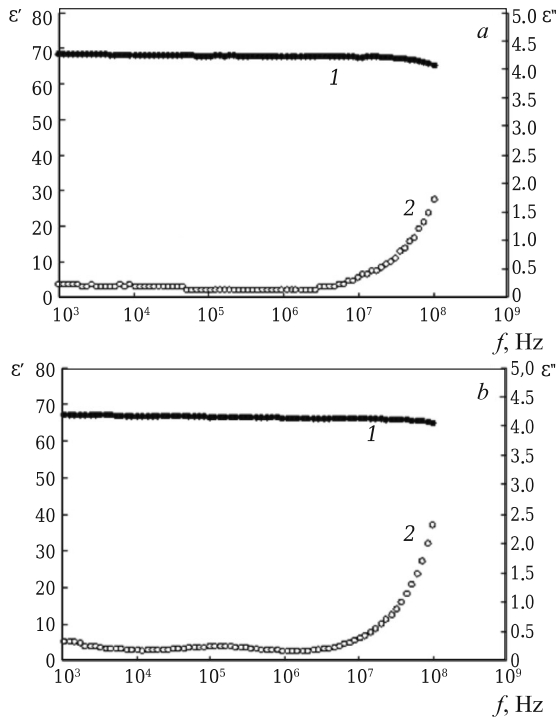


Fig. 7. Frequency dependences of ϵ' (1) and ϵ'' (2) under conditions of through conductivity blocking: *a*) specimen of composition BeO + 30 wt.% TiO₂ (μm); *b*) specimen of composition BeO + 20 wt.% TiO₂ (μm) + 1 wt.% TiO₂ (nano).

capacitances in an experiment the frequency dependence will be mainly recorded for the lower specimen capacitance. Finally, close to the blocking layer for a quarter of the period of the electric field an electric charge will be accumulated and a reverse diffusion current will arise, which will create a non-uniform electric field in the diffusion region. However, considering that ceramic conductivity is low and the diffusion region is limited, frequency dependences obtained in this way for impedance make it possible from simple relationships to calculate some effective capacitance and dynamic conductivity of ceramic and to determine the frequency dependence of the active and imaginary components of dielectric permittivity (Fig. 7).

The actual dielectric permittivity coefficient in the low-frequency region for both ceramic specimens is found within the limits $\epsilon' \approx 68 - 69$ and depends little on frequency. However, these values appear to be an order of magnitude greater compared with the original pure BeO ceramic (without added TiO₂), where $\epsilon' = 6.9 - 7.2$. On this basis it may be proposed that for ϵ' in (BeO + TiO₂)-ceramic the governing effect appears to be addition of TiO₂, not reacting chemically with BeO.

This may be explained by occurrence of additional polarization arising due to presence within the ceramic volume of local conducting regions. Since the through conductivity is blocked, then in an electric field a shift in charges may only proceed within the limits of conducting structures, and at

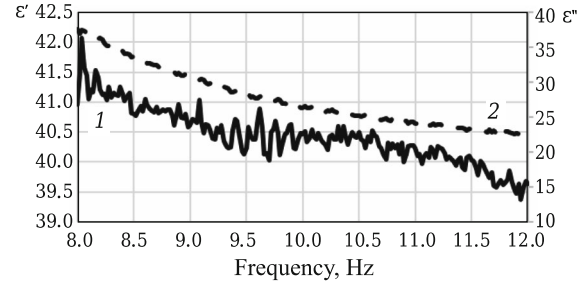


Fig. 8. Change of ϵ' (1) and ϵ'' (2) of a BeO + 30 wt.% TiO₂ (μm) ceramic specimen in the frequency range $(8 - 12) \times 10^9$ Hz.

boundaries of these conducting formations electric charges may be accumulated and apparent additional polarization of the whole volume created. In this case the nature of the distribution of the electric field through a specimen may be strongly inhomogeneous. With an increase in frequency ϵ' there is a reduction, which may be explained by rapid separation of charges into small with respect to size micro- or nanometer TiO₂ particles. An increase in ϵ'' with an increase in frequency is explained by development of intra-cluster relaxation conductivity, when a shift in phase develops between current and voltage.

The method of impedance spectroscopy in the general case covers quite a broad frequency range ($10^3 - 10^9$ Hz). Depending on frequency there is transfer from an ion to a polarization of interaction, which to a significant extent determines the value of dielectric permittivity.

In order to study changes in specimen electrophysical parameters in the case of presence of different types of interaction it was necessary to expand the frequency range $(8 - 12) \times 10^9$ Hz. This choice is due to frequency characteristics of the main regions of using BeO-ceramic in powerful devices for absorption of scattered UHF-radiation. Measurements were made using a standard WR90 wave guide, whose cross section is 23×10 mm. The measurement method used was transfer lines, since it makes it possible to obtain a complex value of dielectric permittivity for ceramic specimens with large losses with an error not exceeding 10%. The method is based on measuring the specimen scattering matrix using a vector circuit analyzer and conversion of the data obtained into complex values of dielectric and magnetic permittivity using NRW software [25, 26]. For this a ZVA50 circuit vector analyzer from Rohde & Schwartz was used.

After calibration. Performed according to the TRL procedure, measurement were made for values of dielectric permittivity for air, which makes it possible to evaluate the level of natural noise of the measurement system in the frequency range $(8 - 12) \times 10^9$ Hz. Differences obtained in results from tabulated values do not exceed 5%, and the minimum value achieved for dielectric loss angle is 0.001.

Then ceramic specimens of the composition BeO + 30 wt.% TiO₂ (μm) 1.47 mm thick were measured (Fig. 8). A reduction is observed in values for a ceramic

specimen compared with ε for low ($10^3 - 10^9$ Hz) values of frequency, obtained from measurements by means of impedance spectroscopy, which points to a change in the reaction mechanism, affecting the change in actual values of dielectric permittivity.

CONCLUSION

Specimens of (BeO + TiO₂)-ceramic containing added TiO₂, having micron sizes without and with addition TiO₂ nano-powder have been prepared. Quite effective mixing of charge components has been demonstrated in a specially developed reactor of the impeller type in distilled water under conditions of continuous bubbling with compressed air. In ceramic specimens with addition of nano-particles TiO₂ structural elements have smaller sizes compared with specimens BeO + TiO₂ where the added TiO₂ had micron sizes.

It has been established by experiment that a specimen of the composition BeO + 20 wt.% TiO₂ (μm) + 1 wt.% TiO₂ (nano) achieves the maximum density at a sintering temperature of 1520°C, which almost coincides with the sintering temperature for a specimen with micron size TiO₂. It has been shown that ceramic specimens exhibit electrical conductivity, which increases in proportion to the angular frequency with a fractional exponent. This has made it possible to intensify the conductivity of a specimens with TiO₂ micro-particles as conductivity of jumpwise type. In a specimen with TiO₂ nano-particles dispersion of conductivity is not observed, and the non-uniform nature of the increase in conductivity in an experiment with an increase in frequency is explained by development relaxation components of current, accompanied by an increase in dielectric losses.

It has been established that $\text{tg}\delta$ for a specimen with TiO₂ micron powder is at a minimum at a frequency $f \sim 1$ MHz, where the reactive component conductivity predominates over the active component. The maximum $\text{tg}\delta$ of this ceramic develops on approach to a frequency of $f \sim 100$ MHz. At this frequency the active conductivity component becomes comparable with the reactive component. However, in a specimen with nano-powder the maximum $\text{tg}\delta$ is at higher frequencies $f > 100$ MHz that points to presence of more significant dielectric loss at high frequencies.

Anomalously high values of ε' and ε'' in a low frequency region are connected with presence of through conductivity and polarization of conducting micro- and nano-clusters, entering into the ceramic structure. Measurements made for the dielectric properties of these ceramics under conditions of blocking through conductivity have made it possible determine approximately actual values ($\varepsilon' \approx 68 - 69$) of dielectric permittivity.

In future in order to improve known volumes of absorbents of UHF energy a detailed study is planned for the effect of a different amount of TiO₂ nano-powder on the

change in ceramic electrical conductivity, its impedance, values of dielectric permittivity, and dielectric loss angle over a wide frequency range $1 \times 10^2 - 12 \times 10^9$, and to establish the change in coefficients for weakening UHF radiation and a standing wave with respect to voltage, determining ceramic capacity to absorb scattered UHF-radiation.

REFERENCES

1. A. S. Edelstein, *Nanoparticles: Synthesis, Properties and Applications*, Philadelphia (1996).
2. V. S. Kiiko, "Effect of adding titanium dioxide on the physicochemical and luminescence properties of beryllium ceramic," *Neorgan. Mater.*, **39**(5), 688 – 693 (1994).
3. R. A. Belyaev, *Beryllium Oxide* [in Russian], Atomizdat, Moscow (1980).
4. V. S. Kiiko, S. N. Shabunin, and Yu. N. Makurin, "Preparation and obtaining physicochemical properties and passage of UHF-radiation by ceramic based on BeO," *Ogneupory Tekhn. Keram.*, No. 10, 8 – 17 (2004).
5. V. S. Kiiko, M. A. Gorbunova, Yu. N. Makarin, et al., "Microstructure and electric conductivity of composite (BeO + TiO₂) ceramics," *Refract. Ind. Ceram.*, **48**(6), 429 – 434 (2007).
6. V. Ya. Vaspapir and V. S. Kiiko, "Beryllium ceramic for contemporary areas of engineering," *Vestn. Vozd.0Kosm. Oboron.*, No. 1(17), 59 – 69 (2018).
7. V. S. Kiiko, "Composite (BeO + TiO₂)-ceramic for electronic engineering and other fields of technology," *Refract. Ind. Ceram.*, **57**, 423 – 426 (2018).
8. A. L. Ivanovskii, V. S. Kiiko, G. P. Akishin, and Yu. N. Makurin, RF patent 2326091. Method for preparing electrically conducting ceramic based on beryllium oxide. Claimant and patent holder GOU VPO UGTU-UPI and IKhTT UrO RAN, Claim 07.10.07; Publ. 06.10.08, Bull. No. 16.
9. M. I. Medvedev, *Scintillation Detectors* [in Russian], Atomizdat, Moscow (1977).
10. M. Landmann, "The electronic structure and optical response of rutile, anatase and brookite TiO₂," *J. Physics Condensed Matter*, **24**(19), 1 – 6 (2012).
11. T. L. Thompson, "Surface science studies of the photo-activation of TiO₂ — new photochemical processes," *Chem. Rev.*, **106**, No. 10, 4428 – 4453 (2006).
12. H. Tang, "Electrical and optical properties of TiO₂ anatase thin films," *J. Appl. Phys.*, **75**, No. 4, 2042 – 2047 (1994).
13. M. V. Kuznetsov, V. S. Kiiko, and A. L. Ivanovskii, "x-ray photo-electron spectroscopy of complex ceramic oxide: BeO–TiO₂–C," *Steklo. Keram.*, No. 10, 16 – 21 (2910)
14. A. V. Ushakov, A. A. Lepeshev, I. V. Karpov, and T. G. Kryshenko, "Physicochemical properties of TiO₂ powder prepared in a Low-pressure plasma-chemical reactor," *Tekhnol. Metall.*, No. 10, 27 – 32 (2012).
15. V. S. Kiiko, Yu. N. Makurin, and A. L. Ivanovskii, *Ceramics Based on Beryllium Oxide: Preparation, Physicochemical Properties, and Applications* [in Russian], UrO RAN, Ekaterinburg (2006).
16. B. A. Belyaev, N. A. Drokin, and V. A. Poluboyarinov, "Study of electrophysical properties of cation substitution ceramic bar-

- ium hexa-aluminate by impedance spectroscopy method,” *Fiz. Tverdogo Tela*, **60**(2), 279 – 275 (2018).
17. J. Ross Macdonald, “Impedance spectroscopy,” *Annals of Bio-medical Engineering*, **20**, 239 – 305 (1992).
 18. D. K. Pradhan, “Studies of dielectric relaxation and AC conductivity behavior of plasticized polymer nanocomposite electrolytes,” *Int. J. Electrochem. Sci.*, **3**, 597 – 608 (2008).
 19. J. C. Dyre, “Universality of AC conduction in disordered solids,” *Reviews of Modern Physics*, **72**(3), 873 – 892 (2000).
 20. V. S. Kiiiko, A. V. Pavlov, and V. A. Bykov, “Preparation and thermophysical properties of BeO ceramic with additions of nano-crystalline titanium dioxide,” *Novye Ogneupory*, No. 11, 57 – 63 (2018).
 21. J. Liu, “Dielectric properties and Maxwell-Wagner relaxation of compounds ACu₃Ti₄O₁₂ (A = Ca, Bi_{2/3}, Y_{2/3}, La_{2/3}),” *J. Appl. Phys.*, **98**, 09370 (2005).
 22. F. Bardi, “Dielectric spectroscopy and conductivity of polyelectrolyte solutions,” *J. Phys. Condens. Matter*, **16**, 1423 – 1463 (2004).
 23. E. A. Nehasheva, O. N. Trubitsyna, N. F. Kartenko, and O. A. Usov, “Ceramic materials for UHF-electronics,” *Fiz. Tverdogo Tela*, **41**(5), 882 – 884 (1999).
 24. A. M. Solodukha and Z. A. Liberman, “Determination of dielectric parameters of ceramic base on dispersion of a complex module,” *Vost. VGU, Ser. Fiz., Matematika*, No. 2, 67 – 71 (2003).
 25. A. I. Malkin, “Dielectric permittivity and permeability measurement system,” *CEUR Workshop Proceedings*, **1814**, 45 – 51 (2017).
 26. A. I. Malkin, N. S. Knyazev, and A. G. Karpov, “Measurement of powder material electrodynamic parameters,” *Metrol. Radio.*, 74 – 78 (2018),